Molecular Docking and Molecular Dynamics of Herbal Plants Phylantus Niruri Linn (Green Meniran) towards of SARS-CoV-2 Main Protease

Jaka Fajar Fatriansyah
Department of Metallurgical and Materials Engineering, Faculty of Engineering, Universitas Indonesia

Syarafina Ramadhanisa Kurnianto
Department of Metallurgical and Materials Engineering, Faculty of Engineering, Universitas Indonesia

Siti Norasmah Surip
Faculty of Applied Sciences, Universiti Teknologi MARA

Agrin Febrian Pradana
Department of Metallurgical and Materials Engineering, Faculty of Engineering, Universitas Indonesia

他

https://doi.org/10.5109/6792822

出版情報：Evergreen. 10 (2), pp.731-741, 2023-06. 九州大学グリーンテクノロジー研究教育センター
バージョン：

Molecular Docking and Molecular Dynamics of Herbal Plants *Phylantus Niruri Linn* (Green Meniran) towards of SARS-CoV-2 Main Protease

Jaka Fajar Fatriansyah[1*], Syarafina Ramadhanisa Kurnianto[1], Siti Norasmah Surip[2], Agrin Febrian Pradana[1], Ara Gamaliel Boanerges[1]

[1]Department of Metallurgical and Materials Engineering, Faculty of Engineering, Universitas Indonesia, Depok, Jawa Barat, Indonesia, 16424

[2]Faculty of Applied Sciences, Universiti Teknologi MARA, 40450 Shah Alam, Selangor, Malaysia

*Author to whom correspondence should be addressed:
E-mail: jakafajar@ui.ac.id

(Received February 11, 2022; Revised May 14, 2023; accepted May 14, 2023).

Abstract: COVID-19 is an infectious disease caused by SARS-CoV-2, which attacks the respiratory tract as the primary target. Until now, no cure for COVID-19 has been found and the efforts made are vaccine distribution, so it is necessary to increase daily human immunity. M^{pro} SARS-CoV-2 is an enzyme for viral replication in host cells so that it can be a target of inhibition. In this study, an in-silico simulation of flavonoid compounds in green meniran plants was carried out: Astragalin, Isoquercitrin, Quercitrin, and Rutin with Quercetin as a control ligand. Predictive analysis of ADMET properties showed that all ligands showed good safety for drug use in humans, except Rutin. The four ligands showed good scores on molecular docking results, which had lower binding scores and MM-GBSA than Quercetin. Molecular dynamics simulation for 20 ns showed that all ligands had good interaction stability, and Quercetin and Isoquercitrin tended to have the most stable interaction. Overall, it was found that Isoquercitrin showed better potential as a M^{pro} SARS-CoV-2 inhibitor with a binding score of -11.973 *kcal/mol*, an average RMSD of 1.652Å, the highest RMSF value of 2.12Å, interacted with 25 protein residues, and had 12 torsions with strain energy of 0.748 *kcal/mol*.

Keywords: SARS-CoV-2, Green Meniran, Flavonoid, SARS-CoV-2 Main Protease, ADMET, Molecular Docking, Molecular Dynamics

1. Introduction

The Coronavirus Disease 2019 (COVID-19) pandemic has been engulfing the world for almost three years. As of November 18, 2021, it has been confirmed that there are 254,847,065 confirmed positive cases worldwide[1)]. COVID-19 is caused by the SARS-CoV-2 virus, which causes respiratory tract infections in humans[2)]. Until now, no drug has been found that can cure COVID-19. WHO has a target for the number of vaccinations to reach 40% by the end of 2021 and 70% by 2022[1)]. With the uneven distribution of vaccinations, many experts predict that the COVID-19 pandemic will become endemic, that is, a condition in which the SARS-CoV-2 virus will continue to circulate, with many people having good immunity through vaccination[3,4,5,6,7)]. So it is necessary to do good remedial techniques to support increased immunity and protection from SARS-CoV-2 in daily activities[8)].

In dealing with COVID-19, the Food and Drug Supervisory Agency of the Republic of Indonesia issued recommendations for guidelines for the use of herbal plants that the public can consume, one of which is green meniran or Phyllanthus niruri Linn[9)]. Green meniran is widely used as a traditional medicine to increase the human body's resistance to antiviral[10)]. Many benefits are produced by meniran because meniran contains several chemical compounds, one of which is flavonoids. Flavonoids can be helpful as antiviral, antioxidant, and immunostimulants which is good for humans[11,12)].

Quercetin, one of the flavonoid compounds, can be a suitable inhibitor of SARS-CoV-2 by inhibiting the Main Protease (M^{pro}) enzyme of SARS-CoV-2[13)]. SARS-CoV-2 depends on M^{pro} to replicate in host cells, so Quercetin can stop the viral replication process[14)]. Astragalin, Isoquercitrin, Quercitrin, and Rutin are flavonoid compounds in green meniran plants[15)]. These compounds are reported to have good antiviral inhibitory abilities in viruses that attack human respiration, so a study was

conducted to see the inhibitory ability of the compounds against SARS-CoV-2 with Quercetin as a positive control.

By conducting this in silico study, it is hoped to be preliminary research and provide recommendations for future experimental tests related to the potential for inhibition of chemical compounds on Phyllantus niruri Linn M^{pro} enzymes from SARS-CoV-2. This study predicted ADMET's properties (Adsorption, Distribution, Metabolism, Excretion, and Toxicity), molecular docking, and molecular dynamics of ligand compounds and protein targets using the Maestro software from Schrödinger. Through this study, an overview of the safety of chemical compounds in green meniran when used on humans will be obtained, and an overview of the mooring and molecular dynamics of green meniran chemical compounds against the M^{pro} target of SARS-CoV-2.

2. Computational method

The material of this research is a three-dimensional structure of the target protein and ligand compounds. The structure of the M^{pro} target protein of SARS-CoV-2 was obtained from the Protein Data Bank website (PDB ID: 7L11), which was obtained based on X-ray diffraction results with a resolution of 1.8[16]. 7L11 was chosen due to similar experiments done with quercetin as ligand control/ligands[17,18]. It was experimentally demonstrated that quercetin could be optimized as an inhibitor. The structure of the ligand compound was obtained from the PubChem website. Prediction of ADMET properties is made using the pkCSM online platform via the http://biosig.unimelb.edu.au/pkcsm/prediction page. The tethering and molecular dynamics simulations were carried out using a computer with a processor of 12 cores and 24 threads, and the application used was Maestro v2018.

2.1 Prediction of ADMET properties on ligands

Prediction is made by entering the SMILES string of the ligand compound and then selecting what properties you want to predict. The molecular properties of each compound will then be used to see the drug-likeness of the ligand compound through Lipinski's Rule of Five and the drug-likeness model score via the https://molsoft.com/mprop/ page.

2.2 Preparation of the three-dimensional structure of the ligand

The ligand structure was prepared and optimized using the ligprep V3.1 feature in the Maestro software. Ligand preparation was carried out using the principle of changing the ligand structure to the most stable 3D structure. Do the removal of salt (desalt) and the addition of hydrogen atoms. Then, the ionization and tautomer processes were carried out using Epik at a pH of 7±2. Energy minimization was carried out using the OPLS-2005 force field, and the conformation with the lowest penalty degree was selected[19].

2.3 Preparation of the three-dimensional structure of the protein

In the M^{pro} SARS-CoV-2 structure with identifier code 7L11, there are two chains, and chain A was chosen to be the target of inhibition in this experiment. The protein structure was prepared using the protein preparation wizard feature in the Maestro software by assigning the bond order, adding hydrogen, missing atoms, and loops to the structure, adding zero-order bonds and disulfide bonds, and removing water from the target protein because it is unwanted in the docking process. Molecular weight, adding suitable ions and tautomer's to the molecule, optimizing hydrogen to prevent clashes, and minimizing structure with RMSD 0.3 using the OPLS-2005 force field model[19].

2.4 Molecular docking

Determination of the grid area with the receptor grid generation feature is carried out to determine the area in the system that acts as a receptor. The grid area is set using the receptor grid generation feature in the Maestro program. At the protein's active site, the grid is regulated with the inhibitory center of XF-1, the native ligand of PDB ID 7L11. We get a grid area with coordinates X = 150.68, Y = 125.21, Z = 233.34 with a box size of 20. Molecular docking in the glide docking feature in the Maestro program. In the Ligand section, the Van der Waals radius is scaled to 1 with a partial charge cutoff of 0.25. The level of precision used for molecular docking is extra precision (XP). The tethered ligand parameters are ligands with more than 500 atomic numbers and more than 100 rotating bonds.

Then, molecular docking was carried out using the Maestro program's glide docking feature. The Desmond function of the maestro program was then used to run a molecular dynamics simulation for 20 ns with a trajectory record of 20 ps using an NPT ensemble.

2.5 Molecular dynamics simulation

The system builder feature is set as shown in Figure 3.10 by setting the solvent with the SPC (water molecule) model in the form of a cubic simulation box. The simulation box is calculated using the buffer method with a distance of a = 10Å, b = 10Å, and c = 10Å. Then minimize the volume of the solvent. In the ions section, it is set to exclude the placement of ions, and the salt is 20Å apart. Added 4Na+ ions for neutralization and 0.15M salt. The system that has been set is then ready for molecular dynamics simulation with the Desmond Molecular Dynamics feature. Molecular dynamics simulation was carried out for 20 ns, with a trajectory record of 20 ps, NPT ensemble[19].

3. Result

3.1 ADMET prediction

Two types of predictions were carried out in predicting the ability of the ligand to become a drug. The first prediction is drug-likeness based on Lipinski's Rule of Five along with the drug-likeness score, shown in Table 1 below. Prediction results from among the five ligands, one ligand can be categorized as a drug according to Lipinski's Rule of Five, namely quercetin, and the other four ligands cannot be classified as a drug. All tested ligands showed positive drug-likeness values for the prediction of the drug-like-ness model score.

Table 1. Lipinski's Rule of Five predictions of each ligand

Ligand	*Lipinski's Rule of Five*		*Druglike-ness Model Score*
	Violation	*Druglike-ness*	
Astragalin	2	*No*	0.67
Isoquercitrin	2	*No*	0.68
Quercetin	0	*Yes*	0.52
Quercitrin	2	*No*	0,82
Rutin	3	*No*	0,91

The second prediction is the prediction of ADMET properties through the pkCSM platform. ADMET prediction results for each ligand compound are attached in Table 2 below. For the absorption properties, most of the ligands met all the parameters except for the Caco2 permeability parameter; the five ligands had a value of less than 0.9. Rutin also did not meet one other absorption parameter, intestinal absorption, with a rate of 23.446%. All ligands met the existing parameters for metabolic properties, which were not substrates & inhibitors of CYP2D6 and CYP3A4 enzymes. Then for excretory properties, all ligands met the current parameters except for Rutin which was classified in the medium category in total clearance. Then, all ligands showed promising results for the nature of toxicity and were not indicated to be toxic in all parameters.

Table 2. ADMET prediction of each ligand

		Astragalin	Isoquercitrin	Quercetin	Quercitrin	Rutin
Absorption	*Water solubility* (log ml/L)	-2.863	-2.925	-2.925	-2.903	-2.892
	Caco2 *permeability* (log Papp: 10^{-6} cm/s)	0.306	0.242	-0.229	0.048	-0.949
	Intestinal absorption (%absorption)	48.052	47.999	77.207	52.709	23.446
	Skin permeability (log Kp)	-2.735	-2.735	-2.735	-2.735	-2.735
	P-glycoprotein I & II inhibitor	*No*	*No*	*No*	*No*	*No*
Distribution	VDss (log L/kg)	1.444	1.846	1.559	1.517	1.663
	Fraction unbound	0.218	0.228	0.206	0.13	0.187
Metabolism	CYP2D6 and CYP3A4 Substrate	*No*	*No*	*No*	*No*	*No*
	CYP2D6 and CYP3A4 Inhibitor	*No*	*No*	*No*	*No*	*No*
Excretion	*Total Clearance* (log ml/min/kg)	0.462	0.394	0.407	0.364	-0.369
	Renal OCT2 substrate	*No*	*No*	*No*	*No*	*No*
Toxicity	AMES *toxicity*	*No*	*No*	*No*	*No*	*No*
	Max. tolerated dose (human) (log mg/kg/day)	0.582	0.569	0.499	0.495	0.452
	hERG I inhibitor	*No*	*No*	*No*	*No*	*No*
	Oral Rat Acute Toxicity (LD50) (mol/kg)	2.546	2.541	2.471	2.586	2.491
	Hepatotoxicity	*No*	*No*	*No*	*No*	*No*
	Skin Sensitisation	*No*	*No*	*No*	*No*	*No*
	Minnow toxicity (log mM)	6.375	8.061	3.721	4.954	7.677

Table 3. Binding site residues of M^{pro} protein with PDB ID 7L11 from the RSCB database

Binding site residues							
1	2	3	4	5	8	14	15
17	18	19	31	69	70	71	72
73	75	95	96	97	102	104	106
107	108	109	110	111	112	119	120
121	122	127	132	150	151	152	153
154	156	157	158	160	200	201	202
203	207	211	213	214	216	218	219
220	221	240	241	242	246	249	250
251	252	253	254	267	270	271	274
275	276	277	279	280	281	282	283
284	286	288	291	292	293	294	295
297	298	299	300	301	303	305	634

3.2 Residue binding site

Determination of the binding site of the M^{pro} protein in this study was done by looking at the database on the RSCB for the 7L11 protein and through the site-map feature of Maestro Schrodinger. Table 3 displays the binding site residue information from the RSCB database, while Table 4 displays the binding site residue information from the site-map feature.

Table 4. Binding site residues of M^{pro} protein with PDB ID 7L11 from *site-map* feature

Native Ligand	Binding site residues						
XF1	25	26	41	49	140	141	142
	143	144	145	163	165	166	187

3.3 Molecular docking results

Results were also acquired from the molecular docking simulation in the form of docking scores with units of kcal/mol. To rank ligands more accurately and determine bond energies, MM-GBSA calculations were also performed. Table 5 below includes the docking scores and MM-GBSA. The compounds with the lowest to highest bonding and free energy scores were Rutin, Isoquercitrin, Quercitrin, Astragalin, and Quercetin. The map of the ligand's interaction with residues is shown in Figure 1.

The docking score validation is conducted in two ways. First, we performed in silico validation by comparing docking score of quercetin, ligand control with other reference[18)], and it was found that the score was close. Second, we compared the performance of quercetin experimentally by in vitro-in vivo studies conducted by[18)]. It was found that quercetin and its derivatives can potentially be 7L11 M^{pro} inhibitors. Further, in the next sub-chapter, we confirm these findings using molecular dynamics simulation.

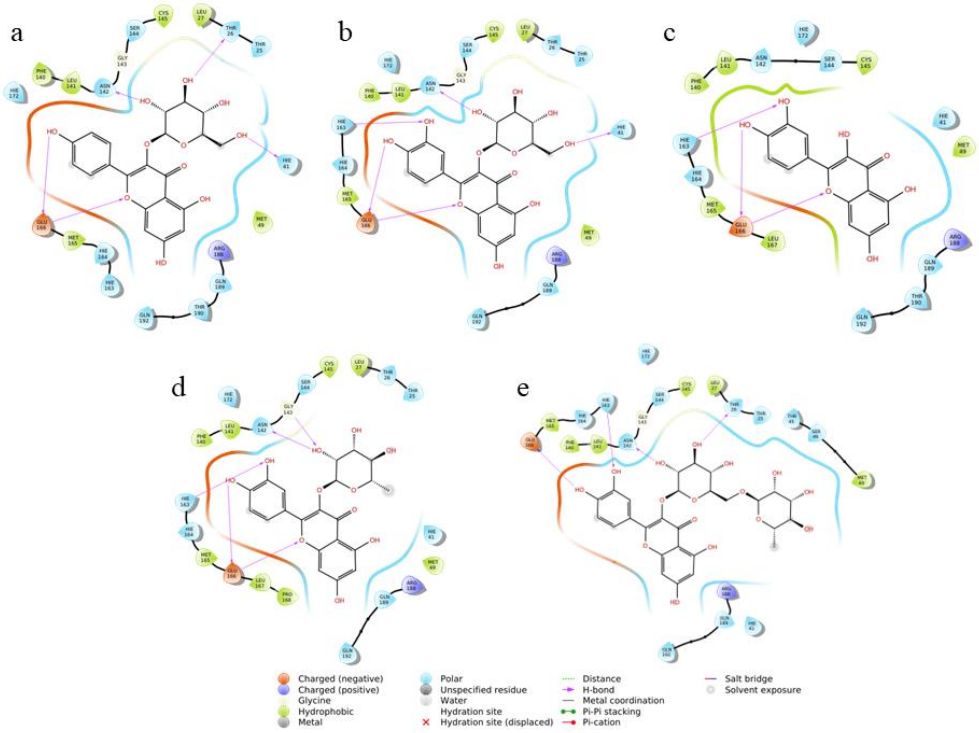

Fig 1. Visualization of ligand interaction (a. Astragalin, b. Isoquercitrin, c.Quercetin, d.Quercitrin, e. Rutin) and residue of M^{pro} protein 7L11

Table 5. Docking scores and MM-GBSA

Ligand	Docking score (kcal/mol)	Bind Energy (MM-GBSA) (kcal/mol)
Rutin	-13.048	-81.84
Isoquercitrin	-11.973	-77.85
Quercitrin	-10.657	-73.67
Astragalin	-10.104	-68.09
Quercetin (control ligand)	-7.972	-54.77

3.4 Molecular dynamic results

3.4.1 Root Mean Square Deviation (RMSD)

Root Mean Square Deviation (RMSD) is used to measure the stability and fluctuation of the protein during the simulation[20] by calculating the change in the average atomic displacement for a certain frame concerning the reference frame. RMSD showed a conformational change of the protein-ligand complex during the simulation, which was 20 ns. The summary of the RMSD results from the interaction of the target protein with the ligand compound can be seen in Table 6 below.

Then a curve fitting was performed to see changes in the RMSD value of each ligand complex with the protein in Figure 2 below.

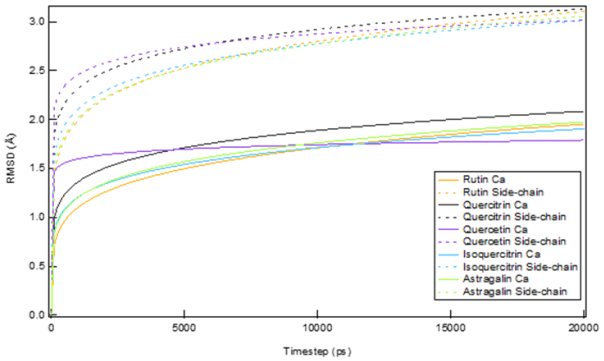

Fig 2. *curve fitting* each RMSD value

Table 6. RMSD result of the molecular dynamics simulation of each ligand with the protein target

	Carbon alpha			*Side Chain*		
Ligand	Lowest Value	Highest Value	Average	Lowest Value	Highest Value	Average
Astragalin	0.813Å	2.604Å	1.73Å	1.394Å	3.547Å	2.711Å
Isoquercitrin	0.874Å	2.484Å	1.652Å	1.329Å	3.43Å	2.691Å
Quercetin	0.766Å	2.301Å	1.722Å	1.255Å	3.309Å	2.821Å
Quercitrin	0.789Å	2.645Å	1.823Å	1.29Å	3.496Å	2.843Å
Rutin	0.864Å	2.587Å	1.641Å	1.341Å	3.562Å	1.718Å

3.4.2 Root Mean Square Fluctuation (RMSF)

Root Mean Square Fluctuation (RMSF) is a movement dynamic that occurs locally in protein residues along the chain. RMSF was used to examine protein-ligand complexes' structural integrity and atomic[19]. In other words, RMSF shows how dynamic the interaction between the protein and ligand is. Similar features can be seen in the RMSF plot of the ligand-protein for each ligand, where the N-terminal and C-terminal residues (start and end) have very high RMSF values because they represent the tails or ends of the protein structure, which are free to move and highly reactive[19]. In the graph, there are peaks representing the protein region that fluctuates the most during the simulation. Residues with an RMSF value greater than 2.5Å exhibit higher mobility and greater fluctuation; thus, residues tend to be less stable[21]. The results of RMSF on the ligand complex with the target protein are attached in Figure 3 and Table 7 below.

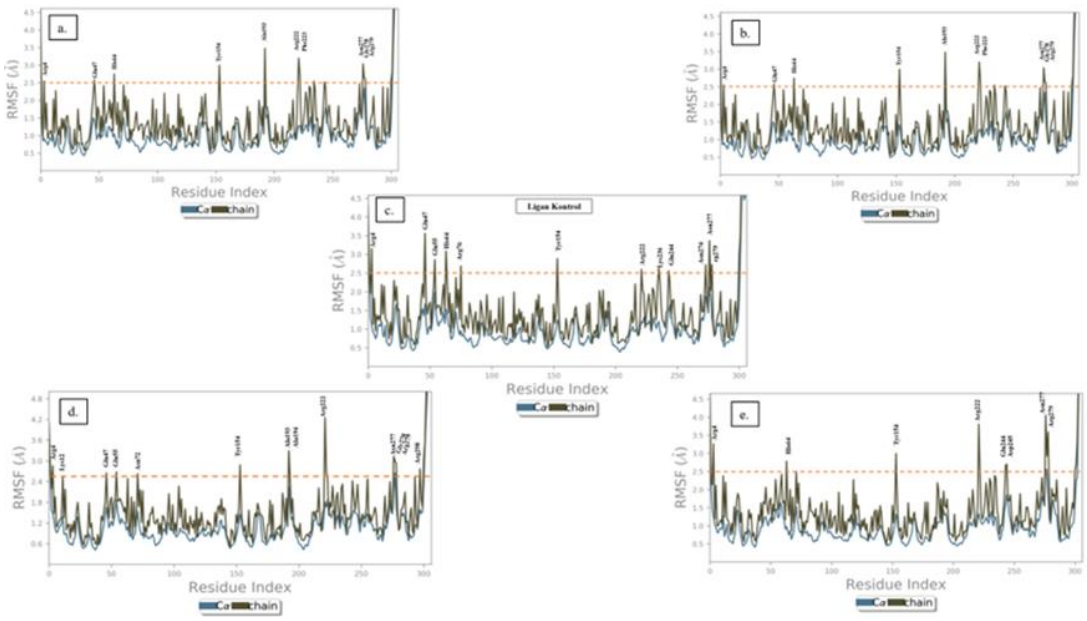

Fig 3. the RMSF graph of molecular dynamics simulation for each ligand with protein Target

Table 7. RMSF result of the molecular dynamics simulation of each ligand with the protein target

	Carbon alpha			Side Chain		
Ligand	**Lowest Value**	**Highest Value**	**RMSF ≥ 2.5Å**	**Lowest Value**	**Highest Value**	**RMSF ≥ 2.5Å**
Astragalin	Cys38 0.43Å	Ala193 2.42 Å	-	Pro39 0.58Å	Ala193 3.48Å	13 residues
Isoquercitrin	Asn28 0.43Å	Asn277 2.12Å	-	Asn28 0.56Å	Asn277 3.08Å	12 residues
Quercetin	Cys38 0.43Å	Asn277 2.12Å	-	Pro39 0.58Å	Glu47 3.56Å	17 residues
Quercitrin	Cys38 0.42Å	Gly278 2.65Å	1 residue	Gly146 0.51Å	Arg22 4.24Å	17 residues
Rutin	Cys38 - 0.41Å	Asn277 - 2.56Å	1 residue	Gly146 0.51Å	Asn277 4.05Å	11 residues

3.4.3 Protein-ligand contact

An interaction diagram displaying the interaction fractions depicts the 20 ns of contact time between the protein and the ligand. The average number of interactions throughout the simulation is known as the interaction fraction. Twenty-seven protein residues interact with the ligand in the Astragalin-protein target complex in Figure 4a during the simulation. The residues Met165, Glu166, and His41 had stable interactions. Additionally, ten protein residues—Thr26, His41, Cys44, Ser46, Gly143, Ser144, Met165, Glu166, Gln189, and Gln192—had an interaction fraction > 0.3 and significantly influenced the interaction between astragalin and protein target. Twenty-five protein residues interact during the simulation in the Isoquercitrin complex with the protein target, as illustrated in Figure 4b. Thr26, Asn142, Met165, Glu166, His41, Gly143, Ser144, Cys145, and Gln192 interact steadily throughout the simulation. Then, eleven protein residues—Thr26, His41, Phe140, Asn142, Gly143, Ser144, Cys145, Met165, Glu166, Gln189, and Gln192—made significant contributions to the complex's interaction. Figure 4c shows the 22 protein residues displayed in the simulation's interaction between quercetin and the protein target. Among these are residues like Met165, Glu166, His41, and His163, whose interactions are likely to be stable. In addition, nine protein residues contributed significantly, namely His41, Phe140, Ser144, Cys145, His163, Met165, Glu166, Arg188, and Gln192. The molecular dynamics results of quercitrin with a protein target display 25 protein residues

interacting with ligands during the simulation, as shown in Figure 4d. Eight protein residues have a stable interaction, namely Thr26, His41, Asn142, Ser144, Cys145, Met165, Glu166, and Arg188. In addition, nine protein residues contribute significantly, namely Thr26, His41, Asn142, Ser144, Cys145, Met165, Glu166, Asp187, and Arg188. The contact interaction between protein and rutin showed 26 interacting protein residues, as shown in Figure 4e. The interactions of the residues Thr26, Asn142, Gly143, Ser144, Cys145, Met165, Glu166, His41, and Arg188 are likely to be stable. Additionally, 15 protein residues—Thr26, His41, Met49, Phe140, Asn142, Gly143, Ser144, Cys145, His163, Met165, Glu166, Asp187, Arg188, Gln189, and Thr190—made significant contributions

3.4.4 Ligand torsion analysis

In molecular dynamics, information regarding ligand torsion is used to determine a ligand's conformational orientation or flexibility when it binds to the target protein. This ligand's flexibility can predict the type of bioactive conformation that typically occurs between the ligand and the target protein during the 20 ns simulation[22,23]. The information about the conformational changes of the ligand torsion during the simulation and the potential torsion value is obtained from the results of the ligand torsion on molecular dynamics. Using the Boltzmann model and equation 1 below, statistical modeling was done to determine the probability of a specific conformation occurring in a chain in the ligand.

$$-\ln N(\tau) = bE(\tau) + b0 \qquad (1)$$

To obtain a linear relationship between the amount of conformation and the potential torsion for each rotatable bond possessed by the ligan, least-square fitting is used[22]. Additionally used a statistical method to estimate the strain energy value (E_s). Strain energy is the quantity of energy required to convert a ligand's conformation from one that is not bound or free to one that is bound or bioactive[24]. Table 7 below shows a summary of the findings of the Boltzmann modeling and the torque information obtained for each ligand.

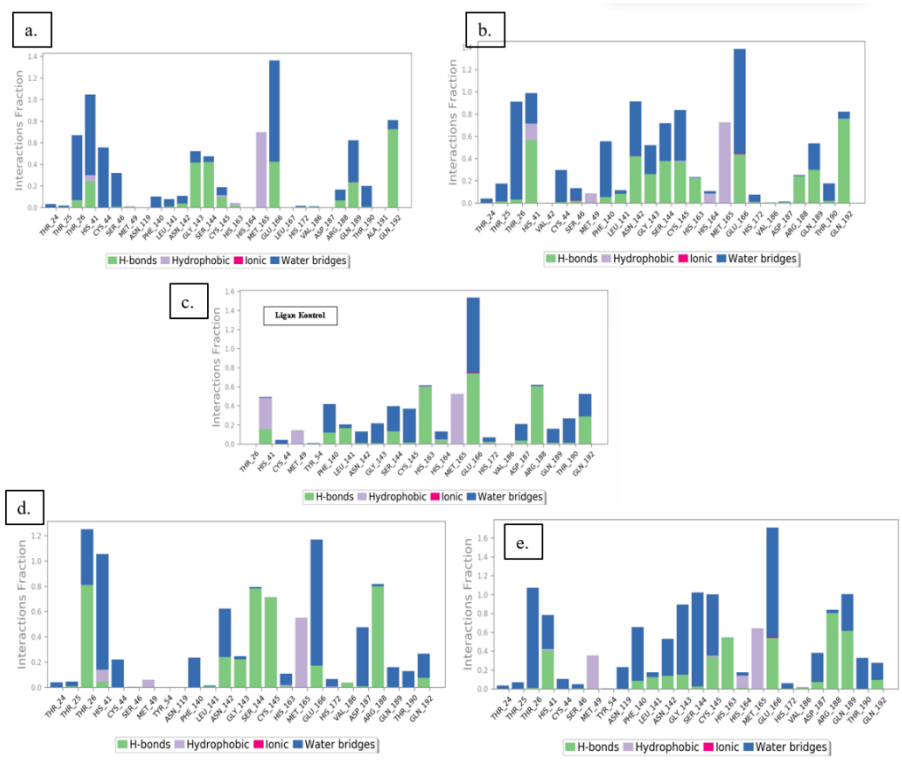

Fig 4. Interaction between protein target and a. Astragalin, b. Isoquercitrin, c. Quercetin, d. Quercitrin, e. Rutin

Table 7. Total of Ligand Torsion and Strain Energy Value

Ligan	Ligand Torsion	b average	E_s1
Astaragalin	10	4.13	0.315
Isoquercitrin	12	1.69	0.748
Quercetin	6	2.51	-0.226
Quercitrin	10	3.55	-0.551
Rutin	16	2.01	0.355

4. Result

4.1 ADMET Prediction

Four ligands, except control ligands, do not meet Lipinski's Rule of Five because they violate more than two of its rules, so they cannot be categorized as drugs. Through the prediction results of the Drug-likeness model score, positive values for each ligand were generated. A positive value indicates the compound can be categorized

as a drug. There is a difference between the drug-likeness score predicted by the Molsoft platform and Lipinski's Rule of Five results. Lipinski's Rule of Five can see the ability of a compound to become a drug based on the prediction of its absorption ability, but it does not apply to natural compounds[25]. Meanwhile, all compounds used as ligands are natural compounds found in green meniran plants.

In the prediction of ADMET properties, for the absorption properties of all ligands, the majority fulfilled all parameters and had results that were classified as having good absorption ability, except for one other parameter so that it was predicted to have low absorption ability in the intestinal mucosa. Rutin also does not meet one other absorption parameter, so it can be concluded that rutin has the most absorption properties. On the nature of distribution, all ligands have results that show they are well distributed in the human body. For metabolic properties, all ligands meet the existing parameters, and their metabolism will not be disturbed. Then for excretory properties, all ligands did not interfere with kidney cleansing function and had a medium total clearance category, except Rutin. Then for the nature of toxicity, all ligands showed good results and were not indicated to be toxic in all parameters.

4.2 Residue Binding Site

A protein's binding site also called a docking site, is an area where molecules can bind to the protein[26]. The location of the binding site on the protein can be known through the complex structure of the protein. The protein's binding site can be used as a reference to see the results of the interactions that occur when the docking simulation and other molecular dynamics are carried out.

4.3 Molecular Docking Results

The docking score and MM-GBS were obtained in Kcal/mol units, where the lower the value, the better the confirmatory ligand bond and bond affinity[27]. Based on the analysis of the molecular docking results that have been carried out, it was found that the Rutin ligand had the best bonding and binding affinity among all ligands, with the highest number of hydroxyl groups, and the lowest docking score and MM-GBSA binding energy, followed by Isoquercitrin, Quercitrin, Astragalin, and Quercetin.

4.4 Molecular Dynamics Result.

4.4.1 Root Mean Square Deviation (RMSD).

The interaction is said to be stable when the RMSD value is below 2.5. The simulation is said to be balanced when the change in the RMSD value towards the end of the simulation is around the thermal average, which is at 1 – 3Å. If there is still fluctuation in the RMSD value outside this range, the simulation is not balanced, and it takes a longer simulation time to get more relevant results.

The RMSD results obtained from the molecular dynamics between all ligands and the target protein have a stable RMSD value of Ca with an average of below 2.5. At the end of the simulation, the RMSD value for Ca is in the range of ±2. To see more clearly the RMSD comparison of each ligand-target protein complex, curve fitting was performed. It was seen that Rutin and Astragalin were the ligands with the most fluctuating RMSD values and tended to be less stable. Isoquercitrin and Quercitrin tended to be more stable, and Quercetin was the ligand with changes, the most stable RMSD among the other four ligands.

4.4.2 Root Mean Square Fluctuation (RMSF)

Residues with RMSF values greater than 2.5Å show higher mobility and more significant fluctuations, so the residue tends to be less stable[28]. In the interaction of the protein with Astragalin, Isoquercitrin, and Quercetin, the RMSF value is more stable because it does not have an RMSF value at Ca that is more than 2.5Å. Meanwhile, one residue on Ca in the interaction of Quercitrin and Rutin with the target protein has an RMSF value greater than 2.5Å. However, overall the residues, which are the binding sites of the protein, have an RMSF value below 2.5Å so that it can be said to have a stable interaction with each ligand.

4.4.3 Protein-Ligand Contact.

This molecular dynamic simulation can illustrate four different forms of interactions: hydrogen interactions, hydrophobic interactions, ionic bonds, and water bridges. Protein and ligand complexes are bound together through a type of interaction called hydrogen interaction. Three kinds of hydrophobic interactions occur: cation bonds, - bonds, and other non-specific interactions. Ionic bonds are interactions between atoms in the range of 3.7A that have opposite charges[29] as opposed to Water Bridges, which is a protein-and-ligand interactions mediated by water molecules and bound by hydrogen interactions.

As a result of the protein target's interaction with the ligand molecule, residues with interaction fractions > 0.3, which play a significant role in the interaction between proteins and ligands, were discovered. Six out of ten residues occur as binding sites in the interaction with astragalin. Nine of the Isoquercitrin's eleven residues occur as protein binding sites interacting with proteins. Interaction of Quercetin with proteins contains protein binding sites on seven of the nine residues. Six of the nine residues involved in the interaction between Quercitrin and proteins are protein binding sites. Additionally, 12 of the 15 residues act as protein-binding sites when rutin interacts with proteins. So, compared to other ligands, Rutin and Isoquercitrin have excellent interactions, especially at the residues at the protein binding site.

4.4.4 Ligand Torsion Analysis

The stability of the conformation that the data from the plot demonstrates the ligand forms. Torsion's potential

value provides information on the possible flexibility of ligands in ligand-protein bonds. The lower the potential value of the torsion possessed by the rotatable bond at an angle, the easier it will be rotatable bond to rotate to that angle[22].

It was predicted that the astragalin ligand would tend to rotate at torsion number 6. Rotation of the Isoquercitrin ligand was most prominent at torsion numbers 1 and 8. The ligand for Quercetin demonstrated a tendency to turn at the torsion number 6. The number 9 torsion is where the quercitrin ligand is most likely to rotate. When binding to the target protein, the Rutin ligand tends to rotate at torsion numbers 2, 9, and 15. The overall energy strain value of the ligand is low, being less than 1 kcal/mol. Therefore, it may be concluded that the ligand does not need to make much effort to change its conformation to become bioactive and bind to the target protein. Quercetin, astragalin, routine, and Isoquercitrin are the ligands with the smallest to the greatest energy strain, respectively.

5. Conclusion

Based on the data and discussion of the research that has been done, several conclusions can be drawn. Prediction of ADMET properties carried out on chemical compounds from green meniran, namely Rutin, Isoquercitrin, Astragalin, Quercetin, and Quercitrin, showed the results that all ligands had good potential to become drugs because of the good properties of ADMET, except Rutin which had less potential because it did not meet three parameters. Rutin, Isoquercitrin, Quercitrin, Astragalin, and Quercetin are the sequence of ligand compounds with docking scores and MM-GBSA from the lowest to the biggest in a row in the results of molecular docking of green meniran plant chemical compounds to the M^{pro} target of SARS-CoV-2.

According to the RMSD results of the molecular dynamics of green meniran plant chemical compounds, the most stable ligand against the M^{pro} target of SARS-CoV-2 was Quercetin. Isoquercitrin is the ligand with the most stable residue interactions, according to RMSF findings. Rutin and Isoquercitrin have several binding site residues that are important in the most prevalent interactions. The average strain energy for all ligands is less than 1 kcal/mol. Overall, upon interacting with the target protein, all of the ligands produced results for molecular dynamics that were comparatively stable. Astragalin, Isoquercitrin, Quercetin, and Rutin have the potential to become SARS-CoV-2 M^{pro} protein inhibitors because they exhibit effects that are comparable to or even superior to those of quercetin, which serves as a control ligand and has been demonstrated to be able to inhibit M^{pro} of SARS-CoV-2. If the projected outcomes of ADMET are also considered, the ligand sequences Quercetin, Isoquercitrin, Quercitrin, Astragalin, and Rutin are predicted to have the best inhibitory qualities and be safe for usage in humans.

Acknowledgments

We thank DRPM UI, which grants us research funds with PUTI Q2 NKB-694/UN2.RST/HKP.05.00/2022.

Data Availability

The data supporting this study's findings are available from the corresponding author upon reasonable request.

References

1) World Health Organization. (2021, November 10). International organizations, vaccine manufacturers take stock of COVID-19 vaccine roll out, share views for 2022. Https://Www.Who.Int/News/Item/10-11-2021-International-Organizations-Vaccine-Manufacturers-Take-Stock-of-Covid-19-Vaccine-Roll-out-Share-Views-for-2022.
2) Pilaquinga, F., Morey, J., Torres, M., Seqqat, R., & Piña, M. de las N. (2021). Silver nanoparticles as a potential treatment against SARS-CoV-2: A review. *Wiley Interdisciplinary Reviews: Nanomedicine and Nanobiotechnology*, **13**(5). https://doi.org/10.1002/wnan.1707
3) Bhatnagar, P., Kaura, S., & Rajan, S. (2020). Predictive models and analysis of peak and flatten curve values of covid-19 cases in india. *Evergreen* Volume **7** Issue 4, 458-467 (2020). https://doi.org/10.5109/4150465
4) Feldscher, K. (2021, August 11). What will it be like when COVID-19 becomes endemic? Https://Www.Hsph.Harvard.Edu/News/Features/What-Will-It-Be-like-When-Covid-19-Becomes-Endemic/.
5) Savanti, F., Setyowati, E., & Hardiman, G. (2022). The Impact of Ventilation on Indoor Air Quality and Air Change Rate. *Evergreen*, Volume **9** Issue 1, 219-225 (2022). https://doi.org/10.5109/4774237
6) Shahriari, B., Hassanpoor, A., Navehebrahim, A., & Jafarinia, S. (2019). A systematic review of green human resource management, *Evergreen*, Volume **6** Issue 2, 177-189 (2019). https://doi.org/10.5109/2328408
7) Yadav, V. K., Yadav, V. K., & Yadav, J. P. (2020). Cognizance on pandemic corona virus infectious disease (covid-19) by using statistical technique: a study and analysis, *Evergreen*, Volume **7** Issue 3, 329-335 (2020) https://doi.org/10.5109/4068611.
8) Sarwar, A., & Imran, M. (2021). Prioritizing infection prevention and control activities for SARS-CoV-2 (COVID-19): a multi-criteria decision-analysis method. *Journal of healthcare leadership*, **13**, 77.
9) Drug and Food Supervisory Agency of the Republic of Indonesia, 2020. Pedoman Penggunaan Herbal dan Suplemen Kesehatan dalam Menghadapi COVID-19 di Indonesia.
10) Nworu, C. S., Akah, P. A., Okoye, F. B. C., Proksch,

P., & Esimone, C. O. (2010). The Effects of Phyllanthus niruri Aqueous Extract on the Activation of Murine Lymphocytes and Bone Marrow-Derived Macrophages. *Immunological Investigations*, **39**(3), 245–267. https://doi.org/10.3109/08820131003599585

11) Kardinan, Ir. A., & Kusuma, F. R. (2004). Meniran Penambah Daya Tahan Tubuh Alami. AgroMedia.
12) Serunting, M. A., Maryana, O. F. T., Syafitri, E., Balqis, S., & Windiastuti, E. (2021). Green Synthesis Silver Nanoparticles (AgNPs) Using Lamtoro Pods Extract (Leucaena leucocephala) and Their Potential for Mercury Ion Detection. *Evergreen*, Volume **8** Issue 1, 63-68 (2021). https://doi.org/10.5109/4372261
13) Bahun, M., Jukić, M., Oblak, D., Kranjc, L., Bajc, G., Butala, M., Bozovičar, K., Bratkovič, T., Podlipnik, Č., & Poklar Ulrih, N. (2022). Inhibition of the SARS-CoV-2 3CLpro main protease by plant polyphenols. *Food Chemistry*, **373**, 131594. https://doi.org/10.1016/j.foodchem.2021.131594
14) Agrawal, P. K., Agrawal, C., & Blunden, G. (2021). Rutin: A Potential Antiviral for Repurposing as a SARS-CoV-2 Main Protease (M^{pro}) Inhibitor. *Natural Product Communications*, **16**(4). https://doi.org/10.1177/1934578X21991723
15) Sarin, B., Verma, N., Martín, J. P., & Mohanty, A. (2014). An overview of important ethnomedicinal herbs of Phyllanthus species: present status and future prospects. *The Scientific World Journal*, *2014*.
16) Zhang, C.-H., Stone, E. A., Deshmukh, M., Ippolito, J. A., Ghahremanpour, M. M., Tirado-Rives, J., Spasov, K. A., Zhang, S., Takeo, Y., Kudalkar, S. N., Liang, Z., Isaacs, F., Lindenbach, B., Miller, S. J., Anderson, K. S., & Jorgensen, W. L. (2021). Potent Noncovalent Inhibitors of the Main Protease of SARS-CoV-2 from Molecular Sculpting of the Drug Perampanel Guided by Free Energy Perturbation Calculations. *ACS Central Science*, **7**(3), 467–475. https://doi.org/10.1021/acscentsci.1c00039
17) Fatriansyah, J. F., Boanerges, A. G., Kurnianto, S. R., Pradana, A. F., & Surip, S. N. (2022). Molecular Dynamics Simulation of Ligands from Anredera cordifolia (Binahong) to the Main Protease (M pro) of SARS-CoV-2. *Journal of Tropical Medicine*, *2022*. https://doi.org/10.1155/2022/1178228
18) Sancineto, L., Ostacolo, C., Ortega-Alarcon, D., Jimenez-Alesanco, A., Ceballos-Laita, L., Vega, S., ... & Santi, C. (2021). L-arginine improves solubility and ANTI SARS-CoV-2 M^{pro} activity of Rutin but not the antiviral activity in cells. *Molecules*, *26*(19), 6062. https://doi.org/10.3390/molecules26196062
19) Fatriansyah, J. F., Rizqillah, R. K., Yandi, M. Y., Fadilah, & Sahlan, M. (2022). Molecular docking and dynamics studies on propolis sulabiroin-A as a potential inhibitor of SARS-CoV-2. *Journal of King Saud University - Science*, **34**(1), 101707. https://doi.org/10.1016/j.jksus.2021.101707
20) Singh, A., & Mishra, A. (2021). Leucoefdin a potential inhibitor against SARS CoV-2 M pro. *Journal of Biomolecular Structure and Dynamics*, **39**(12), 4427–4432. https://doi.org/10.1080/07391102.2020.1777903
21) S. Haider, A. Grottesi, B. A. Hall, F. M. Ashcroft, and M. S. P. Sansom, "Conformational Dynamics of the Ligand-Binding Domain of Inward Rectifier K Channels as Revealed by Molecular Dynamics Simulations: Toward an Understanding of Kir Channel Gating," Biophysical Journal, vol. 88, no. 5, pp. 3310–3320, May 2005, doi: 10.1529/biophysj.104.052019.
22) Hao, M.-H., Haq, O., & Muegge, I. (2007). Torsion Angle Preference and Energetics of Small-Molecule Ligands Bound to Proteins. *Journal of Chemical Information and Modeling*, **47**(6), 2242–2252. https://doi.org/10.1021/ci700189s
23) Krishnaveni, M. (2015). Docking, simulation studies of desulphosinigrin-Cyclin dependent kinase 2, an anticancer drug target Characterization of reproductive gene in marine fish View project. In Int. *J. Pharm. Sci. Rev. Res* (Vol. **30**, Issue 2). https://www.researchgate.net/publication/272792731
24) Z. Fu, X. Li, and K. M. Merz, "Accurate assessment of the strain energy in a protein-bound drug using QM/MM X-ray refinement and converged quantum chemistry," Journal of Computational Chemistry, vol. 32, no. 12, pp. 2587–2597, Sep. 2011, doi: 10.1002/jcc.21838.
25) Bickerton, G. R., Paolini, G. v., Besnard, J., Muresan, S., & Hopkins, A. L. (2012). Quantifying the chemical beauty of drugs. *Nature Chemistry*, **4**(2), 90–98. https://doi.org/10.1038/nchem.1243
26) Gad, E. M., Nafie, M. S., Eltamany, E. H., Hammad, M. S. A. G., Barakat, A., & Boraei, A. T. A. (2020). Discovery of New Apoptosis-Inducing Agents for Breast Cancer Based on Ethyl 2-Amino-4,5,6,7-Tetra Hydrobenzo[b]Thiophene-3-Carboxylate: Synthesis, In Vitro, and In Vivo Activity Evaluation. *Molecules*, **25**(11), 2523. https://doi.org/10.3390/molecules25112523
27) Choudhary, M. I., Shaikh, M., tul-Wahab, A.-, & ur-Rahman, A.-. (2020). In silico identification of potential inhibitors of key SARS-CoV-2 3CL hydrolase (M^{pro}) via molecular docking, MMGBSA predictive binding energy calculations, and molecular dynamics simulation. *PLOS ONE*, **15**(7), e0235030. https://doi.org/10.1371/journal.pone.0235030
28) Haider, S., Grottesi, A., Hall, B. A., Ashcroft, F. M., & Sansom, M. S. P. (2005). Conformational Dynamics of the Ligand-Binding Domain of Inward Rectifier K Channels as Revealed by Molecular Dynamics Simulations: Toward an Understanding of Kir Channel Gating. *Biophysical Journal*, **88**(5), 3310–3320.

https://doi.org/10.1529/biophysj.104.052019
29) Klebe, G. (2013). Protein–Ligand Interactions as the Basis for Drug Action. In Drug Design (pp. 61–88). Springer Berlin Heidelberg. https://doi.org/10.1007/978-3-642-17907-5_4